16th World Conference on Earthquake Engineering, 16WCEE 2017
Santiago Chile, January 9th to 13th 2017
Paper N° 4429
Registration Code: S-J1463344832

An analytical model to predict soil reaction induced by harmonically loaded piles

G. Anoyatis[(1)], G. Mylonakis[(2)], A. Lemnitzer[(3)]

[(1)] *Post Doctoral Scholar, University of California Irvine, Irvine, CA, U.S., ganogiat@uci.edu*
[(2)] *Professor, University of Bristol, Bristol UK, g.mylonakis@bristol.ac.uk; Professor, University of Patras, Rio GR, mylo@upatras.gr*
[(3)] *Assistant Professor, University of California Irvine, Irvine, CA U.S., alemnitz@uci.edu*

Abstract

The theoretical representation of the dynamic horizontal soil reaction to a laterally oscillating pile using an approximate 3D continuum modelling is investigated. The governing elastodynamic equations are reduced by setting the vertical normal stresses in the soil equal to zero. Such a mathematical artifice uncouples the equilibrium in vertical and horizontal directions and allows the solution to be obtained in closed-form. This approximation is physically motivated, and conforms to the presence of a free soil surface and ultimately leads to a weaker dependence of soil response to Poisson's ratio which is in agreement with numerical solutions from literature. This stress condition was not adopted in earlier studies by Tajimi and Nogami and Novak. The stresses and displacements in the soil and the corresponding reaction to a harmonic pile motion are obtained using pertinent eigenvalue expansions over the vertical coordinate. Piles of finite length embedded in a homogenous soil stratum over rigid base are considered. Numerical results are presented in terms of dimensionless parameters and graphs that highlight salient aspects of the problem. A new frequency parameter is introduced to show that the popular dynamic plane-strain model yields realistic values for the soil reaction factor only at high frequencies.

Keywords: piles, lateral loading, soil reaction, elasticity, dynamics, analytical solution

1. Introduction

The degree of accuracy in predicting the lateral response of a pile subject to dynamic loading at the pile head is strongly dependent on the reaction of the surrounding soil. Given its simplicity and versatility, the most well-known model to capture the soil reaction is described in the pioneering work of Baranov [1] and revisited by Novak [2]. The basic model treats the soil medium around the pile as a series of uncoupled incompressible horizontal slices and thus, can be viewed as a plane strain case. Although this model yields soil reactions in closed form, it offers sufficiently reliable predictions in the high frequency range.

To address the limitation identified above, the current study provides a solution that builds upon the work of Tajimi [3] and Nogami and Novak [4]. The pile is considered a solid vertical cylinder and the soil is modelled as a continuum, taking into account all three components of soil displacement under the assumption of zero dynamic vertical normal stresses. This assumption uncouples the equilibrium in vertical and horizontal directions and overcomes the singularities in the important case of incompressible soils, contrary to early studies where the vertical soil displacement was set equal to zero ([5], [3], [4]). A similar approach was adopted in earlier studies ([6], [7]), however, proposed solutions were limited to the kinematic response of laterally-loaded piles. This physically motivated simplification respects the boundary condition of a stress-free soil surface (which is in agreement with numerical solutions found in literature) and reduces the number of governing equations to two – instead of three as found in the classical elastodynamic theory ([8]). The equations of motion in the soil medium are then solved analytically through pertinent eigen-expansions over the vertical coordinate.

Closed-form solutions as a function of pile displacement amplitude are obtained for the stress and displacement field in the soil and the soil reaction to lateral pile motion. The soil reaction is expressed in terms of a dimensionless soil reaction factor which depends on the thickness of the soil layer, soil material damping, Poisson's ratio, excitation frequency and pile diameter. The effect of these parameters on the reaction factor are presented in dimensionless graphs. In the dynamic regime, the real part of the reaction factor describes the stiffness of the soil layer and the imaginary part is associated with a dashpot attached in parallel to the spring. The reaction of the soil layer can be directly employed in the solution of the soil-pile interaction problem based on the boundary conditions at the pile head and tip, and can be then calculated for any given pile displacement profile ([9], [10]). Additional information on the Tajimi model is provided by Chau and Yang [11], Anoyatis [10] and Latini *et al.* [12].

The objective of this study is to: (i) review the dynamic plane strain model of Baranov-Novak and investigate the conditions under which its predictions are realistic; (ii) propose an improved elastodynamic solution for predicting the stress and displacement field in the soil and the reaction at the soil-pile interface for a given harmonic pile motion with an emphasis on the performance at high values of soil Poisson's ratio; and (iii) provide new normalization schemes for soil reaction and frequency that lead to results approaching a single master curve.

2. Proposed Model

The soil-pile system considered is illustrated in Fig. 1: a vertical cylindrical pile is embedded in a homogeneous soil layer overlying a rigid bedrock and is subjected to a harmonic lateral movement $w(z,t) = w(z,\omega)\, e^{i\omega t}$, where t is the time variable, ω is the cyclic excitation frequency and i is the imaginary number ($i = \sqrt{-1}$). The soil layer of thickness H is described by its shear modulus G_s, mass density ρ_s and Poisson's ratio ν_s. The soil is treated as a dissipative material with material damping of the hysteretic type β_s expressed through a complex-valued shear modulus $G_s^* = G_s\,(1 + 2i\beta_s)$.

In cylindrical coordinates the governing elastodynamic equations in the radial and tangential directions are expressed in terms of stresses as

$$\frac{\partial \sigma_r}{\partial r} + \frac{\partial \tau_{rz}}{\partial z} + \frac{1}{r}\frac{\partial \tau_{r\theta}}{\partial \theta} + \frac{1}{r}\left(\sigma_r - \sigma_\theta\right) - \rho_s \frac{\partial^2 u_r}{\partial t^2} = 0 \qquad (1)$$

$$\frac{\partial \tau_{r\theta}}{\partial r} + \frac{\partial \tau_{\theta z}}{\partial z} + \frac{1}{r}\frac{\partial \sigma_{\theta}}{\partial \theta} + \frac{2}{r}\tau_{r\theta} - \rho_s \frac{\partial^2 u_{\theta}}{\partial t^2} = 0 \quad (2)$$

where $u_r = u_r(r,\theta,z,t)$ and $u_\theta = u_\vartheta(r,\theta,z,t)$ are the horizontal and tangential components of soil displacement, $\sigma_r = \sigma_r(r,\theta,z,t)$ and $\sigma_\theta = \sigma_\theta(r,\theta,z,t)$ are the normal stresses acting along r and θ directions, respectively; $\tau_{rz} = \tau_{rz}(r,\theta,z,t)$ is the shear stress along z and perpendicular to r; $\tau_{r\theta} = \tau_{r\theta}(r,\theta,z,t)$ is the shear stress along θ and perpendicular to r; and $\tau_{\theta z} = \tau_{\theta z}(r,\theta,z,t)$ is the shear stress along z and perpendicular to θ.

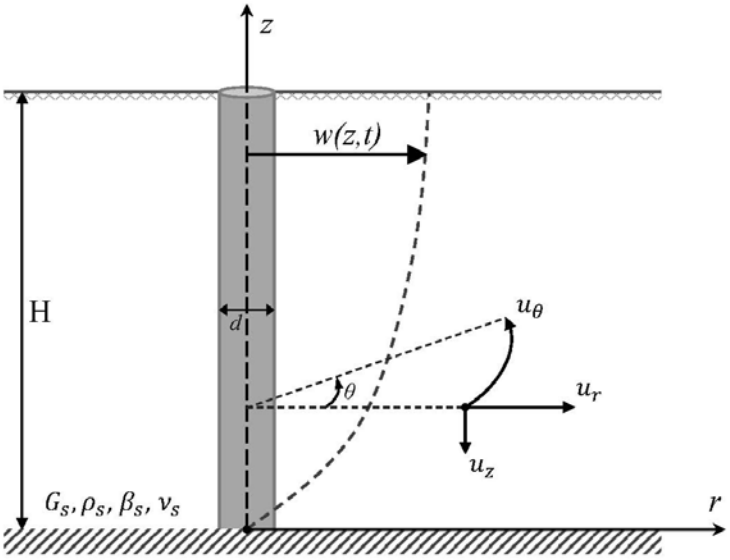

Fig. 1 – Problem considered

Taking into account stress-strain relations and considering harmonic soil response of the form $u_r = u_r(r,\theta,z,\omega)\, e^{i\omega t}$ and $u_\theta = u_\theta(r,\theta,z,\omega)\, e^{i\omega t}$, Eqs. (1) and (2) can be rewritten in terms of displacements in the following elaborate form

$$\eta_s^2 \frac{\partial}{\partial r}\left[\frac{1}{r}\left(\frac{\partial (r u_r)}{\partial r} + \frac{\partial u_\theta}{\partial \theta}\right)\right] - \frac{1}{r^2}\frac{\partial}{\partial \theta}\left[\frac{\partial (r u_\theta)}{\partial r} - \frac{\partial u_r}{\partial \theta}\right] + \frac{\partial^2 u_r}{\partial z^2} + \left(\frac{\omega}{V_s^*}\right)^2 u_r = 0 \quad (3)$$

$$\frac{\partial}{\partial r}\left[\frac{1}{r}\left(\frac{\partial (r u_\theta)}{\partial r} - \frac{\partial u_r}{\partial \theta}\right)\right] + \eta_s^2 \frac{1}{r^2}\frac{\partial}{\partial \theta}\left[\frac{\partial (r u_r)}{\partial r} + \frac{\partial u_\theta}{\partial \theta}\right] + \frac{\partial^2 u_\theta}{\partial z^2} + \left(\frac{\omega}{V_s^*}\right)^2 u_\theta = 0 \quad (4)$$

where $V_s^* = V_s\sqrt{1+2i\beta_s}$ is the complex valued propagation velocity of shear waves in the soil.

In Eqs. (3) and (4) η_s is a dimensionless compressibility coefficient which is merely a function of soil Poisson's ratio and is associated with the effect of vertical soil displacement on stresses. Herein η_s emerges from the assumption of $\sigma_z = 0$, which complies with a stress-free soil surface and leads to finite vertical displacement ($u_z \neq 0$):

$$\eta_s = \sqrt{\frac{2-\nu_s}{1-\nu_s}} \quad (5)$$

The alternative assumption of normal strain $\varepsilon_z = 0$ (i.e., $u_z = 0$) adopted by the study of Nogami and Novak [4] leads to the following expression for the compressibility factor

$$\eta_s = \sqrt{\frac{2\left(1-\nu_s\right)}{1-2\nu_s}} \tag{6}$$

A problem arising from the use of this equation is the sensitivity to Poisson's ratio, as η_s becomes infinitely large when ν_s approaches *0.5*. A more thorough discussion is presented in Anoyatis *et al.* [13].

To uncouple the set of partial differential equations (Eqs. 3 and 4), the horizontal and tangential displacements are expressed in terms of two potential functions $\mathbf{\Phi}$ and $\mathbf{\Psi}$ following a degenerate Helmholtz decomposition scheme ([8]) as shown below

$$u_r = \frac{\partial \mathbf{\Phi}}{\partial r} + \frac{1}{r}\frac{\partial \mathbf{\Psi}}{\partial \theta} \tag{7}$$

$$u_\theta = \frac{1}{r}\frac{\partial \mathbf{\Phi}}{\partial \theta} - \frac{\partial \mathbf{\Psi}}{\partial r} \tag{8}$$

Substituting Eqs. (7) and (8) in (3) and (4) leads to the following new set of uncoupled differential equations

$$\eta_s^2 \nabla^2 \mathbf{\Phi} + \frac{\partial^2 \mathbf{\Phi}}{\partial z^2} + \left(\frac{\omega}{V_s^*}\right)^2 \mathbf{\Phi} = 0 \tag{9}$$

$$\nabla^2 \mathbf{\Psi} + \frac{\partial^2 \mathbf{\Psi}}{\partial z^2} + \left(\frac{\omega}{V_s^*}\right)^2 \mathbf{\Psi} = 0 \tag{10}$$

where $\nabla^2 = \frac{\partial^2}{\partial r^2} + \frac{1}{r}\frac{\partial}{\partial r} + \frac{1}{r^2}\frac{\partial^2}{\partial \theta^2}$ is the Laplacian operator.

Using the method of separation of variables the potential functions $\mathbf{\Phi}$ and $\mathbf{\Psi}$ can be expressed as products of three functions i.e., $\mathbf{\Phi}(r,\theta,z) = R_1(r)\,\Theta_1(\theta)\,Z_1(z)$ and $\mathbf{\Psi}(r,\theta,z) = R_2(r)\,\Theta_2(\theta)\,Z_2(z)$. This leads to the decomposition of the partial differential equations (Eqs. 9 and 10) into three ordinary differential equations in r, θ and z ([13])

$$\frac{d^2R}{dr^2} + \frac{1}{r}\frac{dR}{dr} - \left(q^2 + \frac{n^2}{r^2}\right)R = 0 \tag{11}$$

$$\frac{d^2\Theta}{d\theta^2} + n^2\Theta = 0 \tag{12}$$

$$\frac{d^2Z}{dz^2} + a^2 Z = 0 \tag{13}$$

from which it arises that

$$q = \frac{1}{\eta_s}\sqrt{a^2 - \left(\frac{\omega}{V_s^*}\right)^2} \tag{14}$$

where a and n are positive real numbers; q has dimensions of 1 / Length and can be viewed as a wavenumber for radially propagating waves.

When obtaining the general solutions to Eqs. (9) – (11) ([10]), the potential functions are written as follows

$$\mathbf{\Phi} = \left[\, A_1\, I_n(qr) + B_1\, K_n(qr) \,\right]\left[A_2 \sin n\theta + B_2 \cos n\theta\right]\left[A_3 \sin az + B_3 \cos az\right] \tag{15}$$

$$\Psi = \left[A_4 I_n(q\eta_s r) + B_4 K_n(q\eta_s r)\right]\left[A_5 \sin n\theta + B_5 \cos n\theta\right]\left[A_6 \sin az + B_6 \cos az\right] \quad (16)$$

where $I_n()$ and $K_n()$ are the first and second kind modified Bessel functions of the *n-th* order, respectively. A_i, B_i $(i = 1, 2, 3, \dots, 6)$ are constants to be determined from the boundary conditions of the problem. For $r \to \infty$ constants A_1 and A_4 must vanish to ensure bounded response. Constants A_2 and B_5 must also vanish to satisfy the conditions of zero radial and tangential displacement, u_r and u_θ, at $\theta = \pi/2$ and $\theta = 0$, respectively. The above are valid for $n = 1$. The additional conditions of zero soil displacement at the base of the soil layer and stress-free soil surface enforce $A_3 = A_6 = 0$ and $\cos aH = 0$ which, in turn, yields $a_m = (\pi/2H)(2m - 1)$, $m = 1, 2, 3, \dots$. a_m are the eigenvalues of the boundary-value problem with $a_1 < a_2 < a_3 \dots < a_N$ (N being the number of modes employed in the analysis).

Considering the above, Eqs. (13) and (14) are rewritten as

$$\Phi_m = B_2 \cos\theta\, K_1(q_m r) \sin a_m z \quad (17)$$

$$\Psi_m = A_5 \sin\theta\, K_1(q_m \eta_s r) \sin a_m z \quad (18)$$

Each eigenvalue a_m corresponds to a unique eigenfunction $\Phi_m(z)$ (i.e., soil mode) which is called the *m-th* fundamental solution which is expressed as

$$\Phi_m(z) = \sin a_m z \quad (19)$$

These modes have the important property of orthogonality described mathematically as follows

$$\int_0^H \Phi_k(z)\,\Phi_m(z)\,dz = 0, \qquad m \neq k \quad (m,\, k = 1,\, 2,\, 3,\, \dots) \quad (20)$$

It is anticipated that the solution should be obtained by the superposition of all modes. Thus soil displacements u_r and u_θ can be expressed as an infinite sum of Fourier terms including the soil modes Φ_m and a term $U_{r,\theta\, m}$. The latter is a frequency-dependent term associated with the spatial variable r only. Accordingly,

$$u_{r,\theta} \propto \sum_{m=1}^{\infty} U_{r,\theta m}(r,\omega)\,\Phi_m(z) \quad (21)$$

Since soil modes form an orthogonal set (Eq. 20), pile displacement *w* can be expressed through a normal-mode expansion similar to soil response (Eq. 21)

$$w(z,\omega) = \sum_{m=1}^{\infty} W_m(\omega)\,\Phi_m(z) \quad (22)$$

where W_m [units of Length] are frequency-varying coefficients.

Substituting Eqs. (17) and (18) into (5) and (6) and imposing compatibility of displacements at the soil-pile interface [i.e., $u_r(d/2, 0, z, \omega) = w(z, \omega)$ and $u_\theta(d/2, \pi/2, z, \omega) = -w(z, \omega)$] and taking into account the orthogonality of soil modes (Eq. 20), soil displacements are expressed as

$$u_r(r, \theta, z, \omega) = \cos\theta \sum_{m=1}^{\infty} U_{rm}(r,\omega)\, W_m(\omega)\, \Phi_m(z) \quad (23)$$

$$u_\theta(r, \theta, z, \omega) = \sin\theta \sum_{m=1}^{\infty} U_{\theta m}(r,\omega)\, W_m(\omega)\, \Phi_m(z) \quad (24)$$

where

$$U_{r\,m}(r,\omega) = B_m\left[s_m K_0(q_m r) + \left(\frac{d}{2r}\right)K_1(q_m r)\right] - A_m\left(\frac{d}{2r}\right)K_1(q_m \eta_s r) \tag{25}$$

$$U_{\theta\,m}(r,\omega) = B_m\left(\frac{d}{2r}\right)K_1(q_m r) - A_m\left[s_m \eta_s K_0(q_m \eta_s r) + \left(\frac{d}{2r}\right)K_1(q_m \eta_s r)\right] \tag{26}$$

and A_m, B_m being the dimensionless constants

$$A_m = \frac{2K_1(s_m) + s_m K_0(s_m)}{s_m K_0(s_m)K_1(s_m\eta_s) + s_m\eta_s K_0(s_m\eta_s)\left[s_m K_0(s_m) + K_1(s_m)\right]} \tag{27}$$

$$B_m = \frac{2K_1(s_m\eta_s) + s_m\eta_s K_0(s_m\eta_s)}{s_m K_0(s_m)K_1(s_m\eta_s) + s_m\eta_s K_0(s_m\eta_s)\left[s_m K_0(s_m) + K_1(s_m)\right]} \tag{28}$$

In the above equations $s_m = q_m\ d/2$ (Eq. 12) is a dimensionless frequency-dependent parameter.

3. Soil Reaction Factor

The horizontal soil reaction p along the soil-pile interface, resulting from the pile motion is expressed as ([4])

$$p(z,\omega) = -\int_0^{2\pi}\left[\sigma_{r,0}\cos\theta - \tau_{r\theta,0}\sin\theta\right](d/2)\ d\theta \tag{29}$$

where $\sigma_{r,0} = \sigma_r(d/2,\theta,z,\omega)$ and $\tau_{r\theta,0} = \tau_{r\theta}(d/2,\theta,z,\omega)$ are the radial normal and shear stresses, respectively, acting at the pile periphery.

For the problem at hand the soil reaction p can be written in the alternative form in terms of series expansion:

$$p(z,\omega) = \pi G_s^* \sum_{m=1}^{\infty} R_m^*(\omega) W_m(\omega)\Phi_m(z) \tag{30}$$

where R_m^* is a complex valued soil reaction factor associated with the *m-th* soil mode

$$R_m^* = s_m^2\ \frac{\eta_\sigma^2\left[2K_1(s_m\eta_s) + s_m\eta_s K_0(s_m\eta_s)\right]K_1(s_m) + \eta_s^2\left[2K_1(s_m) + s_m K_0(s_m)\right]K_1(s_m\eta_s)}{s_m K_0(s_m)K_1(s_m\eta_s) + s_m\eta_s K_0(s_m\eta_s)\left[s_m K_0(s_m) + K_1(s_m)\right]} \tag{31}$$

and η_s is denoted as the secondary compressibility coefficient

$$\eta_\sigma = \sqrt{\frac{2}{1-\nu_s}} \tag{32}$$

In the solution of Nogami and Novak [4] the reaction factor R_m^* is obtained from Eq. (31) using $\eta_\sigma = \eta_s$, where η_s is given from Eq. (6). In both solutions the soil reaction factor depends on soil parameters (i.e., $\nu_s, \beta_s, \rho_s, G_s$), the excitation frequency ω and on only one pile parameter, which is the pile diameter d.

In dynamic conditions the complex valued soil reaction factor can be cast in the equivalent forms $R_m^* = Real(R_m^*) + i\ Imaginary(R_m^*)$ or $R_m^* = R_m(1 + 2i\beta_m)$: $R_m = Real(R_m^*)$ is the dynamic stiffness and $2\beta_m R_m(\omega) = Imaginary(R_m^*)$ is the corresponding loss stiffness. The parameter $\beta_m = Imaginary(R_m^*)\ /\ 2Real(R_m^*)$ defines an equivalent damping ratio, which is analogous to the percentage of critical damping in a simple oscillator ([14]). $R_m = R_m(\omega)$ can be interpreted as a frequency dependent spring and $2\beta_m R_m(\omega)/\omega$ as a dashpot attached in parallel to the spring.

4. Plane Strain model

The Baranov-Novak ([1], [2]) soil restraining action against the horizontal pile motion can be expressed in an analogous manner through a complex valued reaction factor R^*

$$R^* = s^2 \frac{4K_1(q)K_1(s) + sK_1(q)K_0(s) + qK_0(q)K_1(s)}{qK_0(q)K_1(s) + sK_1(q)K_0(s) + qsK_0(q)K_0(s)} \tag{33}$$

where s and q are dimensionless frequency parameters given by the following expressions

$$s = \frac{ia_0}{2\sqrt{1+2i\beta_s}} \quad \text{and} \quad q = \frac{s}{\eta_s} \tag{34a, b}$$

and $a_0 = \omega d/V_s$ is a dimensionless frequency and η_s is obtained from Eq. (6).

The basic assumption of the dynamic plane strain model eliminates the vertical strains and shear strains on the plane perpendicular to the pile axis. This means that only an incompressible horizontal soil slice of the soil medium is considered. The plane strain reaction factor R^* cannot capture the layer resonances as it does not consider the thickness of the soil layer and therefore exhibits an asymptotic behavior for $\omega \to 0$ (Figs. 4, 6). Accordingly, the model cannot capture static stiffness. This is not the case for a pile of finite length embedded in a soil stratum overlying a stiff base. On the other hand, R^* can be viewed as mathematically accurate for an infinitely-long pile embedded in a half space and subjected to uniform lateral displacement along its whole length. The present solution can be reduced to the plane strain by eliminating the variation of soil displacements in the vertical direction (i.e., setting $a = 0$ in Eqs. 13 and 14). Despite its simplicity, the plane strain model yields realistic predictions for frequencies beyond cutoff (see ensuing discussion for Fig. 6). Thus, it can be viewed as a special case of the proposed more complete solution, restricted to frequencies beyond cutoff. This is an inherent weakness of the plane strain model, its assumptions being valid only after wave propagation initiates in the medium.

5. Discussion of numerical results

The effects of pile length and soil mode on the static soil reaction factor are investigated in Fig. 2. It is observed that for a given L/d, higher values of R_m correspond to higher modes. This trend is more pronounced for short piles ($L/d < 10$) where the reaction factor pertaining to the *10-th* mode is approximately five times higher than the value for the *1-st* mode. Comparison with the solution of Nogami and Novak [4] shows that the results of that study are higher than those obtained from the proposed model. The divergence is stronger with decreasing pile length and higher modes – the maximum difference being observed for $L/d = 5$ and $m = 10$.

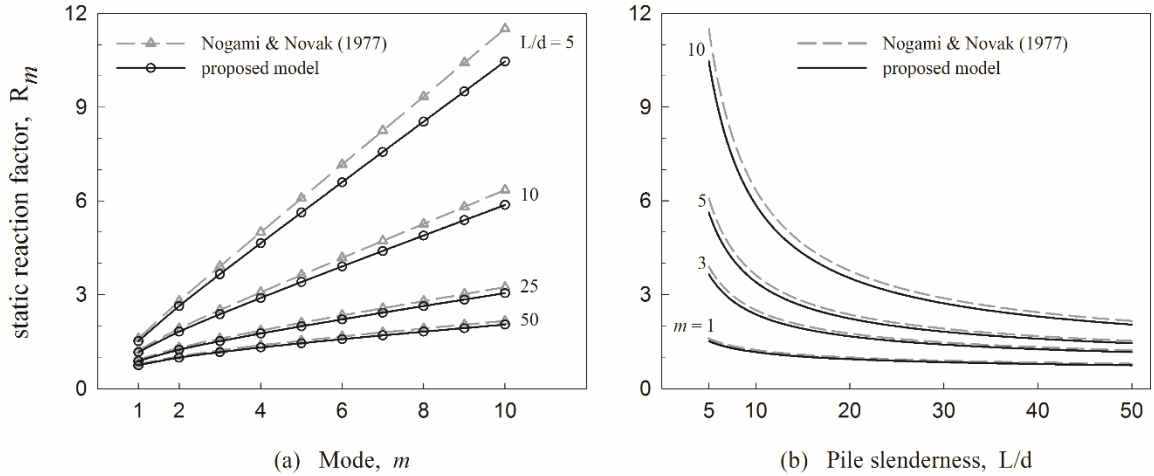

(a) Mode, m (b) Pile slenderness, L/d

Fig. 2 – Effect of modes and pile slenderness on static soil reaction factor

The effect of Poisson's ratio on the static reaction factor is investigated for two selected modes in Fig. 3. It is shown that higher values of v_s always correspond to higher R_m for the range of pile lengths considered. As anticipated, the lower the Poisson's ratio the better the agreement with the predictions of the earlier study.

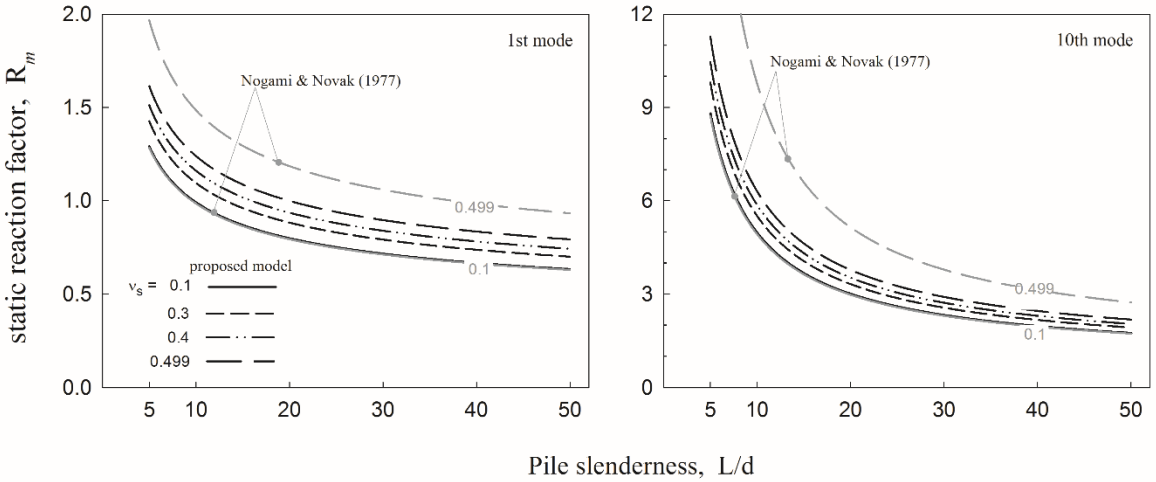

Fig. 3 – Effect of Poisson's ration on static soil resistance factor

Results for the soil reaction factor in the dynamic regime obtained from the proposed solution are presented in Figs. 4 – 6. The solution of Nogami and Novak [4] is added for comparison. Different representations of the soil reaction factor and frequency are employed, which shed light into the physics of the problem. Some general trends are observed: For each mode *m*, the dynamic soil reaction factor (i.e., real part of soil reaction) decreases with increasing frequency up to the *m-th* resonance, while for the same frequency range, damping (i.e., imaginary part of soil reaction) is practically unaffected by frequency and depends solely on the soil material damping (since only "weak" travelling waves associated with the *m-th* mode develop in the medium). At *m-th* resonance the dynamic reaction R_m attains a local minimum, which is associated with a distinct jump in damping due to energy radiation, as horizontally travelling waves emerge in the soil medium.

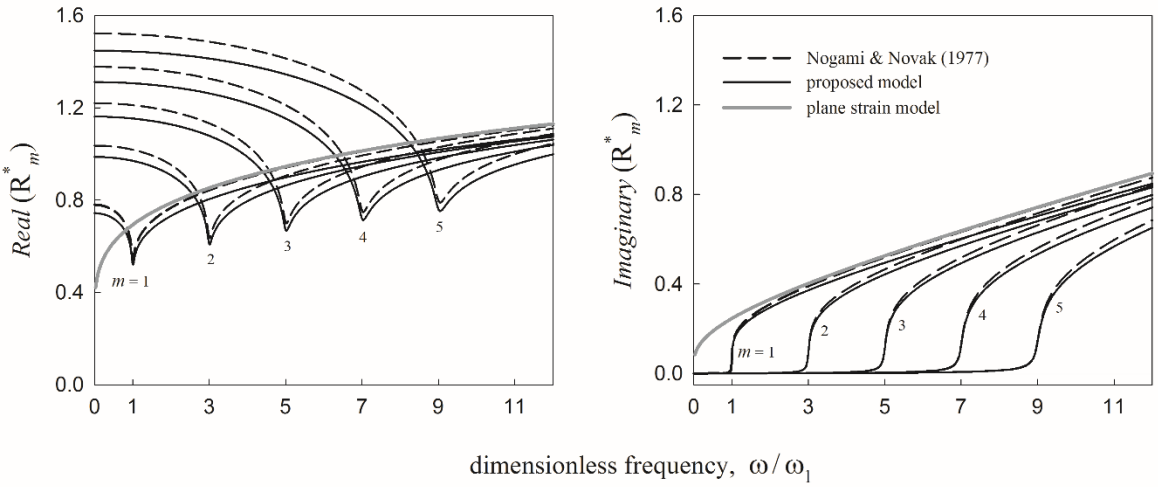

Fig. 4 – Variation of real and imaginary part of soil reaction with frequency for selected modes. Comparison with Nogami and Novak [4] and the plane strain model; $H/d = 50$, $\beta_s = 0.01$

The variation of the real and the imaginary part of dynamic soil reaction with frequency for the first five modes pertaining to a long pile is shown in Fig. 4. The frequency is normalized by the first resonant frequency of the system, ω_1. A strong dependence of stiffness (i.e., real part of soil reaction) on the oscillation mode is observed below the resonant frequency, while at the same frequency range the damping (i.e., imaginary part of soil reaction) is practically unaffected by frequency and is controlled by soil material damping. With increasing frequency the dynamic reaction factor becomes gradually independent of soil mode, with all curves practically converging to a single curve at high frequencies. As anticipated, results from the study of Nogami and Novak [4] are always higher than those of the proposed model.

A perhaps better representation for frequencies in the range $0 < \omega < \omega_m$ is illustrated in Fig. 5, where the frequency is normalized by a different value for each mode, namely, the *m-th* resonant frequency for the *m-th* propagating mode. It is shown that for dynamic soil reaction all results collapse to a single curve. Also, damping is practically constant and controlled by soil material damping.

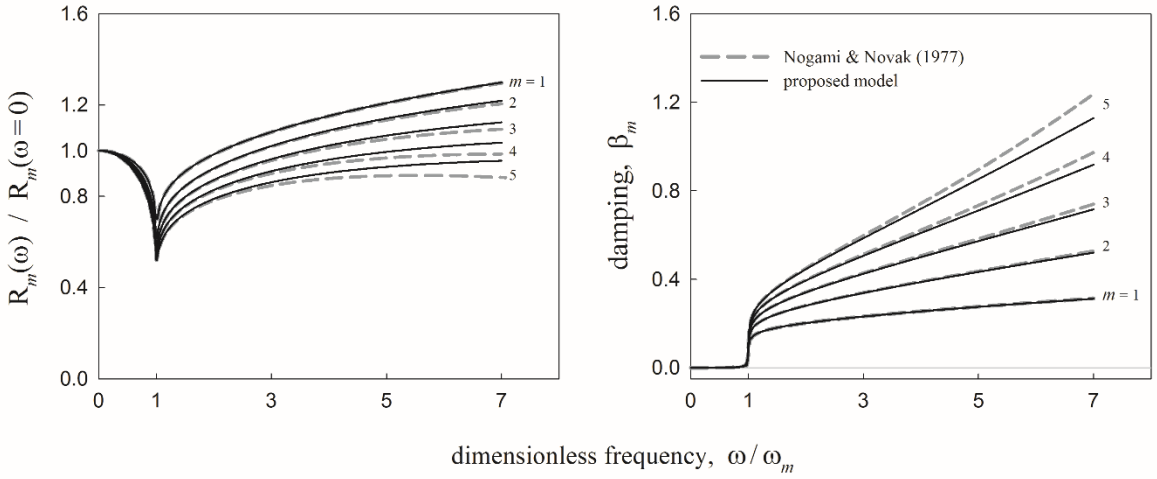

Fig. 5 – Variation of dynamic soil reaction and damping with frequency for selected modes. Comparison with Nogami and Novak [4]; $H/d = 50$, $\beta_s = 0.01$

The effect of soil layer thickness on the soil reaction factor of a damped medium is presented in Fig. 6, where only the first mode is taken into account. Note that different dimensionless parameters are used for the frequency below and beyond resonance: $a_0 = \omega d/V_s$ being the familiar dimensionless frequency parameter and $a_{cutoff,m} = \omega_m d/V_s$ being the cutoff frequency of each mode or the *m-th* resonance. It is suggested that: (i) below cutoff ($\omega < \omega_m$) spring and dashpot are best represented in the forms $R_m(\omega)/R_m(\omega = 0)$ and β, as functions of $a_0/a_{cutoff,m}$; (ii) beyond cutoff ($\omega > \omega_m$), stiffness is best represented in the form $R_m(\omega)$ and both parameters as a function of the dimensionless frequency function $\left(a_0^2 - a_{cutoff,m}^2\right)^{1/2}$. Note that the latter parameter has been successfully employed in the representation of vertical soil reaction in high frequencies for the case of an axially-loaded pile in a homogeneous stratum [15]. It has not been explored in the lateral mode.

For frequencies below *m-th* resonance all stiffness curves in Fig. 6(a) start from unity, as the dynamic stiffness is normalized with its static value ($\omega = 0$), and decreases monotonically with frequency. Over the same frequency range, damping is independent of frequency (Fig. 6a) and practically equals the soil material damping, i.e., all damping curves converge to a single curve before resonance. Beyond the cutoff frequency, waves start to propagate in the medium resulting in a sudden increase in damping. It is shown that the dynamic stiffness becomes insensitive to the soil thickness H (Fig. 6b). This is an anticipated behavior, since the waves emitted from the periphery of the oscillating pile tend to spread out in a horizontal manner without regard for the vertical dimension ([16], [17]). This wave radiation pattern explains the very good agreement observed between the plane strain model and the more rigorous solution.

For frequencies below cutoff, longer piles or thicker strata always correspond to higher values of dynamic soil reaction factor; whereas for the damping coefficient all curves practically converge. For frequencies beyond cutoff all curves converge into a single curve and the soil reaction can be well captured by the plane strain model.

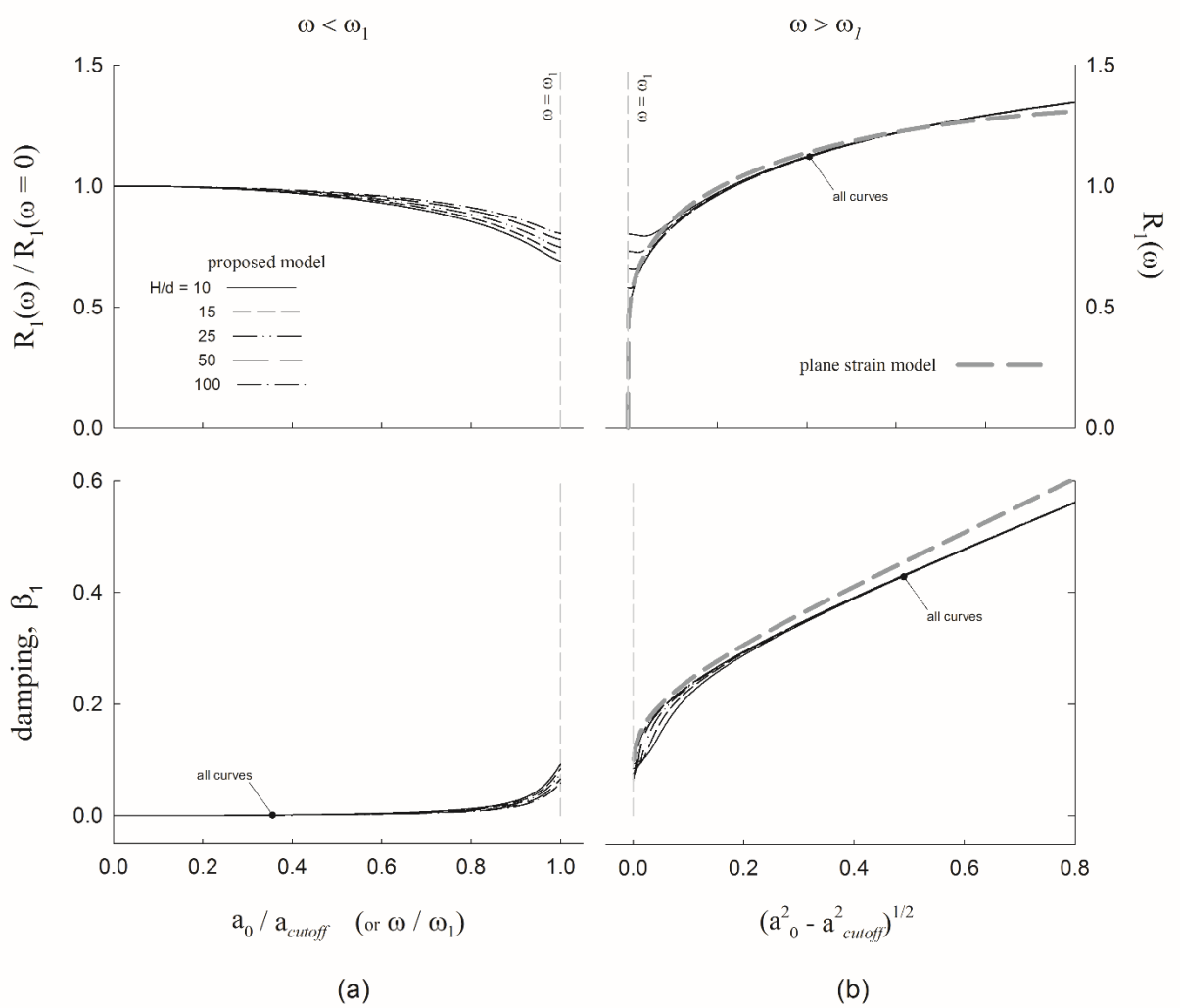

Fig. 6 – Effect of pile slenderness on soil reaction in dynamic regime; $\beta_s = 0.05$, $\nu_s = 0.4$

6. Conclusions

An approximate three-dimensional analytical solution is derived for the reaction of a homogeneous soil layer to a laterally oscillating pile. The proposed approach allows a closed form solution to be obtained as a function of an arbitrary pile motion for the stress and displacement field in the soil and the associated horizontal reaction at the soil-pile interface. The main findings of this study can be summarized as follows:

a) Fundamental to this study is that the vertical normal stress in soil σ_z is zero. This approximation is compatible with the existence of a free soil surface and leads to a finite vertical soil displacement. This overcomes the sensitivity of earlier models to Poisson's ratio for nearly incompressible soils.

b) A dimensionless incremental frequency parameter $\left(a_0^2 - a_{cutoff,m}^2\right)^{1/2}$ was introduced for describing the soil reaction in the high frequency range ($a_m > a_{cutoff,m}$). This representation allows the reaction factor to exhibit the same behavior regardless of actual soil layer thickness, value of Poisson's ratio, soil material damping and oscillation mode.

c) It was found that the dynamic soil reaction factor below cutoff frequency is best normalized by the corresponding static stiffness ($\omega = 0$) as a function of dimensionless frequency ratio $a_0/a_{cutoff,m}$. Beyond the cutoff frequency, the dynamic stiffness can be best normalized by the soil's shear modulus and is best expressed as a function of the frequency $\left(a_0^2 - a_{cutoff,m}^2\right)^{1/2}$. These properties stem from the dependence of the solution on the cutoff frequency of each mode and the gradual transformation of the wave field with increasing frequency beyond resonance, from three-dimensional to two-dimensional.

d) It was also observed that with increasing frequency the plane strain solution converges to the more rigorous solution. However, significant discrepancies in stiffness appear, especially for short piles, for frequencies below cutoff.

6. References

[1] V. Baranov, "On the calculation of an embedded foundation. Voprosy Dinamiki i Prochnosti.," *polytech.Inst.Riga, Latvia. ,* vol. 14, pp. 195-209, 1967.

[2] M. Novak, "Dynamic Stiffness and Damping of Piles," *Canadian Geotechnical Journal,* vol. 11, no. 4, pp. 574-598, 1974.

[3] H. Tajimi, "Dynamic analysis of a structure embedded in an elastic stratum," in *4th World Conference on Earthquake Engineering*, Santiago, Chile, 1969.

[4] T. Nogami and M. Novak, "Resistance of soil to a horizontally vibrating pile," *Earthquake Engineering and Structural Dynamics,* vol. 5, no. 3, pp. 249-261, 1977.

[5] H. Matsuo and S. Ohara, "Lateral earth pressures and stability of quay walls during earthquakes," in *2nd World Conference on Earthquake Engineering, Vol. I*, Tokyo, 1960.

[6] A. Veletsos and A. Younan, "Dynamic soil pressures on rigid cylindrical vaults," *Earthquake Engineering and Structural Dynamics,* vol. 23, no. 6, pp. 645-669, 1994.

[7] A. Veletsos and A. Younan, "Dynamic modeling of response of rigid embedded cylinders," *J. Eng. Mech.,* vol. 121, no. 9, pp. 1026-1035, 1995.

[8] K. Graff, Wave Motion in Elastic Solids., Dover Publications, 1975.

[9] M. Novak and T. Nogami, "Soil-pile interaction in horizontal vibration," *Earthquake Engineering & Structural Dynamics,* vol. 5, no. 3, pp. 263-281, 1977.

[10] G. Anoyatis, "Contribution to kinematic and inertial analysis of piles by analytical and experimental methods," PhD thesis, University of Patras, Rio, Greece, 2013.

[11] K. Chau and X. Yang, "Nonlinear interaction of soil-pile in horizontal vibration," *Journal of Engineering Mechanics,* vol. 131, no. 8, pp. 847-858, 2005.

[12] C. Latini, V. Zania and B. Johannesson, "Dynamic stiffness and damping of foundations for jacket structures," in *6th International Conference on Earthquake Geotechnical Engineering*, Christchurch, New Zealand, 2015.

[13] G. Anoyatis, G. Mylonakis and A. Lemnitzer, "Soil Reaction to Lateral Harmonic Pile Motion," *Soil Dynamics and Earthquake Engineering,* vol. 87, p. 164–79, 2016.

[14] R. W. Clough and J. Penzien, Dynamics of Structures, New York: McGraw Hill, 1993.

[15] G. Anoyatis and G. Mylonakis, "Dynamic Winkler modulus for axially loaded piles," *Geotechnique,* vol. 62, no. 6, pp. 521-536, 2012.

[16] G. Gazetas and G. Mylonakis, "Seismic soil-structure interaction: New evidence and emerging issues.," *Spec. Publ. No. 75, ASCE,* pp. 1110-1174, 1998.

[17] G. Mylonakis, "Elastodynamic model for large-diameter end-bearing shafts," *Journal of the Japanese Geotechnical Society: Soils and Foundations*, vol. 41, no. 3, pp. 31-44, 2001b.